JOURNAL OF VIROLOGY, Jan. 1995, p. 430–438 Vol. 69, No. 1
0022-538X/95/$04.00+0

Viral RNA Modulates the Acid Sensitivity of Foot-and-Mouth Disease Virus Capsids

STEPHEN CURRY,[1]† CHARLES C. ABRAMS,[1] ELIZABETH FRY,[2] JOHN C. CROWTHER,[1] GRAHAM J. BELSHAM,[1] DAVID I. STUART,[2,3] AND ANDREW M. Q. KING[1]*

Pirbright Laboratory, Institute for Animal Health, Pirbright, Surrey, GU24 0NF,[1] Laboratory of Molecular Biophysics, Oxford University, Oxford OX1 3QU,[2] and New Chemistry Laboratory, Oxford Centre for Molecular Sciences, Oxford OX1 3QT,[3] United Kingdom

Received 13 July 1994/Accepted 13 October 1994

Foot-and-mouth disease virus (FMDV) manifests an extreme sensitivity to acid, which is thought to be important for entry of the RNA genome into the cell. We have compared the low-pH-induced disassembly in vitro of virions and natural empty capsids of three subtypes of serotype A FMDV by enzyme-linked immunosorbent assay and sucrose gradient sedimentation analysis. For all three subtypes (A22 Iraq 24/64, $A10_{61}$, and A24 Cruzeiro), the empty capsid was more stable by 0.5 pH unit on average than the corresponding virion. Unexpectedly, in the natural empty capsids used in this study, the precursor capsid protein VP0 was found largely to be cleaved into VP2 and VP4. For picornaviruses the processing of VP0 is closely associated with encapsidation of viral RNA, which is considered likely to play a catalytic role in the cleavage. Investigation of the cleavage of VP0 in natural empty capsids failed to implicate the viral RNA. However, it remains possible that these particles arise from abortive attempts to encapsidate RNA. Empty capsids expressed from a vaccinia virus recombinant showed essentially the same acid lability as natural empty capsids, despite differing considerably in the extent of VP0 processing, with the synthetic particles containing almost exclusively uncleaved VP0. These results indicate that it is the viral RNA that modulates acid lability in FMDV. In all cases the capsids dissociate at low pH directly into pentameric subunits. Comparison of the three viruses indicates that FMDV A22 Iraq is about 0.5 pH unit more sensitive to low pH than types $A10_{61}$ and A24 Cruzeiro. Sequence analysis of the three subtypes identified several differences at the interface between pentamers and highlighted a His–α-helix dipole interaction which spans the pentamer interface and appears likely to influence the acid lability of the virus.

Picornaviruses possess an icosahedral capsid made up of 60 copies of each of four proteins: three surface proteins, VP1 to VP3, and a smaller internal protein, VP4. In the case of foot-and-mouth disease virus (FMDV), which is the most sensitive of all the picornaviruses to acidic conditions, this structure dissociates at pH values below neutrality into pentamers containing five copies of VP1 to VP3, releasing in the process the viral RNA and VP4 (10, 13, 55). Although detrimental to the virus in vitro, acidic conditions may in fact enable infection in vivo. It has been postulated that a process of receptor-mediated endocytosis, in which FMDV uncoats because of acidification of the endosome, may provide a pathway into the cytosol for the virus genome (5, 15, 16).

For a number of membrane-enveloped viruses (e.g., Semliki Forest virus and influenza virus), it is well established that the low-pH environment of endosomes plays a role in virus infection (see reference 45). Acidification of the endosome activates a fusion protein in the viral lipid envelope, causing fusion with the endosomal membrane and leading to release of the nucleocapsid into the cytosol.

Picornaviruses, including FMDV, lack a lipid envelope but face the same problem of cell membrane penetration. Although receptor-mediated endocytosis is an attractive model for picornavirus cell entry, the evidence remains controversial. Electron microscopy studies have identified poliovirus in coated pits, vesicles, and early endosomal compartments of infected cells (65, 66). However, evidence from electron microscopy also suggests direct penetration of the membrane by this virus (25). Experiments using weak bases or ionophores which raise the endosomal pH have shown that these agents inhibit infection by poliovirus (43, 66), human rhinovirus (HRV) (49), and FMDV (5, 15, 16). In the case of poliovirus, however, more recent work has cast doubt on the role of endosomal acidification in the infection pathway (33, 52). HRV and FMDV are both more sensitive to disruption by acidic conditions, and the best available evidence suggests that this sensitivity is important for infection. For example, Pérez and Carrasco (52) showed that an antibiotic which specifically inhibits vacuolar proton-ATPases, thus perturbing endosomal pH, had no effect on poliovirus infection of HeLa cells but inhibited infection by HRV. Most recently, evidence has been presented to suggest that the acidic conditions within late endosomes are responsible for the uncoating of HRV (53). Mason et al. compared the abilities of monoclonal antibody-coated poliovirus and FMDV to infect Chinese hamster ovary cells expressing the Fc receptor and found that only FMDV could infect by this route (46). This difference may be related to the fact that poliovirus undergoes a conformational change upon interaction with its normal cellular receptor (37), which appears to be a prerequisite for successful infection (29). FMDV, by contrast, is structurally unaffected by its receptor, and once internalized, its capsid rapidly dissociates into pentamers (6). The results of studies by Mason and his coworkers (46) are thus consistent with the supposed role of endosomal acidification in FMDV infection, although further work is required to demonstrate this rigorously.

In the meantime, there has been considerable interest in the

* Corresponding author. Phone: (483) 232441. Fax: (483) 232448.
† Present address: Department of Biological Chemistry and Molecular Pharmacology, Harvard Medical School, Boston, MA 02115.

structural basis of the effect of pH on picornaviruses. For these studies, a wealth of structural data obtained by high-resolution X-ray crystallography is available. The determination of a type O FMDV structure (2) highlighted a clustering of histidine residues ($pK_a = 6.8$) at the interpentamer interface, which may be involved in pH-induced structural changes in the vicinity of pH 7. Crystal structures have also been determined for at least one strain of poliovirus (35), HRV (58), and mengo virus (42). A variety of approaches have been used to study the effects of acid. X-ray crystallographic techniques have been used to determine acid-induced structural changes in mengo virus (38) and HRV (31). Amino acid changes which affect acid lability have been identified by the generation and sequencing of acid stable mutants of HRV (31, 63) and FMDV (12). Another approach involved computer modelling of the effects of pH on electrostatic interactions within poliovirus and HRV (64).

We have compared in quantitative detail the acid sensitivities of three type A strains of FMDV. The differences observed are discussed in light of sequence comparisons and the newly determined crystal structure (to be presented in detail elsewhere) of one of the type A viruses. We have also investigated the acid lability of empty capsids of FMDV, for which a crystal structure has also recently been obtained (22). These particles, lacking the genomic RNA, are a natural product of infection by several strains of FMDV, notably those of type A. As classically described for picornaviruses, natural empty capsids differ from the capsids of mature virions in possessing precursor protein VP0, in place of VP2 and VP4. The cleavage of VP0 normally accompanies RNA encapsidation, and we were curious to determine the effects of both processes, VP0 cleavage and RNA encapsidation, on capsid stability. We have therefore compared the acid lability of FMDV with that of two forms of empty capsid, one containing exclusively uncleaved VP0 and the other a novel type of empty particle that we have observed in the three different type A strains, which lacks RNA yet contains predominantly the cleavage products VP2 and VP4 (21). The results of this comparative study are presented and interpreted with reference to the new structural data.

MATERIALS AND METHODS

Virus purification. Although the methods used for purification of viruses and empty capsids contain only slight variations from established protocols, we will describe them briefly because of the unusual nature of some of our results.

FMDV subtypes $A10_{61}$, A22 Iraq 24/64, and A24 Cruzeiro (Brazil 55) were used. A22 Iraq 24/64 was the gift of E. Ouldridge (Pittman-Moore), and A24 Cruzeiro was supplied by Pfizer. Viruses and empty capsids were produced by infecting BHK-21 cell monolayers. Upon attaining full cytopathic effect (CPE), the cells were detached by shaking, pooled along with the growth medium (3% [vol/vol] adult bovine serum, 5% [vol/vol] tryptose phosphate broth, 92% [vol/vol] Eagles minimal essential medium [MEM]), and lysed by the addition of 0.1% (vol/vol) Triton X-100 at 4°C. Purification was achieved in essentially the same way as described previously (11, 59). Briefly, this involved precipitation of proteinaceous material with 50% saturated ammonium sulfate, ultracentrifugation of the redissolved precipitate onto a sucrose cushion, and finally, ultracentrifugation through a 15 to 45% sucrose gradient. All sucrose solutions contained 40 mM sodium phosphate–100 mM NaCl (pH 7.6) (buffer P). After the final step of purification, the peak fractions of virions and natural empty capsids were pooled separately and stored at −80°C between experiments. The concentrations of these pools were determined by combining spectrophotometric measurements with optical densitometry of Coomassie blue-stained sodium dodecyl sulfate (SDS)-polyacrylamide gels.

Radiolabelled viruses and empty capsids were prepared in the following manner. Flasks (25 cm^2) of BHK-21 monolayers were inoculated with 1 to 10 PFU per cell for 30 min at 37°C. The inoculum was replaced by viral growth medium for a further 30 min at 37°C. For the next hour, the cells were washed at 20-min intervals with Eagle's MEM lacking methionine and/or cysteine. At 2 h postinfection, up to 37 MBq of L-[^{35}S]methionine or ^{35}S-Protein Labeling Mix (NEN Research Products) was added. The cells were harvested upon attaining greater than 80% CPE (usually 3.5 to 6 h postinfection) by pouring off the growth medium and lysing the monolayers with 0.5 ml 1% (vol/vol) Nonidet P-40 (NP-40) in buffer P. Cell debris was pelleted, and the supernatant was treated with 0.1 mg of RNase per ml for 5 min before centrifugation through a 12-ml 10 to 30% (wt/vol) sucrose gradient containing buffer P for 125 min at 12°C and 261,000 × *g* to separate the virus and empty capsids. The gradient was drained into fractions of equal volume. Peak fractions were identified by determining the radioactivity in 10-μl samples blotted onto filter paper and immersed in scintillant.

In experiments to label viral RNA, BHK-21 cells were treated with 1.25 μg of actinomycin D per ml for 30 min prior to infection with $A10_{61}$ FMDV. The inoculum was allowed to adsorb for 30 min at 37°C before being replaced by viral growth medium containing 1.25 μg of actinomycin D per ml. At 2 h postinfection, 25 MBq of [^{3}H]uridine was added. The cells were harvested after a further 2 h, and the labelled lysate was centrifuged and analyzed by scintillation counting as described above.

Quantification of VP0 content of empty capsids from autoradiograms. For the calculation of the number of VP0 molecules per empty capsid from autoradiograms of L-[^{35}S]methionine-labelled capsids analyzed on SDS-polyacrylamide gels, it is assumed that (i) $N_{VP0} + N_{VP2} = 60$ and (ii) $N_{VP1} = N_{VP3} = 60$, where N_{VP1}, N_{VP2}, and N_{VP3} are the numbers of VP1, VP2, and VP3 molecules per capsid. The integrated absorbance, A_{VP0} (determined by optical densitometry), of a VP0 band on the autoradiogram can be expressed as follows:

$$A_{VP0} = kM_{VP0}N_{VP0} \quad \text{(I)}$$

where M_{VP0} is the number of methionines in VP0 and k is an arbitrary constant. Equation (I) can be re-expressed as follows:

$$k = \frac{A_{VP0}}{M_{VP0}N_{VP0}} \quad \text{(II)}$$

The integrated absorbance of the bands containing VP1, VP2, and VP3 (which are not well resolved by the densitometer) is:

$$A_{VP123} = k(M_{VP1}N_{VP1} + M_{VP2}N_{VP2} + M_{VP3}N_{VP3}) \quad \text{(III)}$$

By substituting equation II for k in equation III and applying the assumptions listed above, it is possible to obtain the following expression of the number of VP0 molecules per empty capsid:

$$N_{VP0} = \frac{60A_{VP0}(M_{VP1} + M_{VP2} + M_{VP3})}{(M_{VP2}A_{VP0} + M_{VP0}A_{VP123})} \quad \text{(IV)}$$

which can be evaluated by using known sequence and optical densitometer data.

Purification of empty capsids expressed by vaccinia virus recombinant. A recently developed vaccinia virus recombinant (vT7CA2) provided an alternative source of empty capsids of $A10_{61}$ FMDV (1). The vector, which will be described in detail elsewhere, contained the capsid coding region (P1) for FMDV and the viral proteases 2A and 3C under the control of the bacteriophage T7 promoter, recombined into the vaccinia virus thymidine kinase gene by using an insertion plasmid containing the T7 promoter and termination signals derived from plasmid pAR2529 (30). The inserted genes were expressed in infected human TK^- 143 cells coinfected with a vaccinia virus recombinant, vTF7-3, encoding the T7 polymerase (30) (vTF7-3 and pAR2529 were gifts of B. Moss) as follows: 850-cm^2 plastic roller bottles of human TK^- 143 cells were infected with 5 ml of vTF7-3 and 5 ml of harvested vTF7-3 and 5 ml of vT7CA2 for 1 h. Growth medium (50 ml; Eagle's MEM containing 10% [vol/vol] fetal calf serum, 0.4% [wt/vol] sodium carbonate-bicarbonate, 2 mM L-glutamine [pH 7.0]) was then added. Full CPE was obtained after 16 to 24 h. The cells were detached, pooled, and pelleted at 4°C. The pellet was dispersed in 1% (vol/vol) NP-40 containing buffer T (50 mM Tris, 100 mM NaCl, 2 mM $MgCl_2$ [pH 7.6]). Unresuspended material was removed by centrifugation. FMDV empty capsids and other proteins were pelleted onto a 30% sucrose cushion containing buffer T by centrifugation of the supernatant at 142,000 × *g* for 3 h at 12°C. This pellet was resuspended in buffer T and treated with 0.2% (vol/vol) NP-40–0.1 mg of RNase per ml. Unresuspended material was pelleted, and the supernatant was centrifuged through a 10 to 30% sucrose gradient containing a 0.75-ml 45% sucrose cushion, both containing buffer T, for 3 h at 275,000 × *g* and 12°C. The analysis of fractions by SDS-polyacrylamide gel electrophoresis (PAGE) identified those which contained empty capsids.

Radiolabelled capsids were prepared from the vaccinia virus recombinants by a simpler protocol. Monolayers (25 cm^2) of TK^- 143 cells were infected with 10 μl each of the two recombinants (described above). When CPE was judged to be around 80% (usually after 16 h), the growth medium was removed, and every 20 min for an hour the cells were washed in Eagle's MEM lacking methionine and cysteine. Up to 37 MBq of ^{35}S-Protein Labeling Mix was added, and the cells incubated at 37°C for a further 2 h. The medium was then poured off, and the cells were washed gently with cold phosphate-buffered saline (PBS). Lysis was achieved by adding 0.4 ml of 1% (vol/vol) NP-40 in buffer T for 5 min. The cell debris was pelleted, and the supernatant was treated with 0.1 mg of RNase per ml for 5 min and centrifuged in the same way as described above for unlabelled capsids. Fractions containing the capsids were identified by scintillation counting as described above.

pH treatment. The pH sensitivities of virions and empty capsids of FMDV

were investigated by diluting a small volume of sample in low-pH buffers. After a set time, the pH was restored to pH 7.6, and the samples were analyzed by one of two methods: enzyme-linked immunosorbent assay (ELISA) or sucrose gradient sedimentation. The 50 mM sodium phosphate or sodium acetate buffers were prepared across the pH range of 5.3 to 7.6 by mixing 0.5 M stock solutions of the acidic (A) and basic (B) forms of the salts in different proportions (so that A + B = 2 ml) and diluting the mixtures to 20 ml. The buffers also included 50 or 250 mM NaCl, 0.1% (vol/vol) Tween 20 (for ELISA experiments) or 0.1% (vol/vol) NP-40 (for sedimentation experiments), 3 mM NaN_3, and 2.5 μM phenol red. To prepare samples for ELISA analysis, one volume of antigen was diluted into 49 volumes of pH buffer; in sedimentation analysis experiments one volume of virus or capsids was diluted into 9 volumes of buffer. In both cases the pH of the treatment was measured after inclusion in the pH buffer of the appropriate proportion of the solution in which the virus or empty capsid had been stored. After 8 min at the lower pH at 21°C, the pH of the buffer was restored by the addition of an appropriate neutralization solution. Neutralization solutions were prepared for each pH buffer by mixing opposite proportions (i.e., B + A) of the appropriate acidic and basic stock solutions and adding 0.33 ml of 2 M NaOH. The volume of this solution required to restore the pH to 7.6 was determined empirically (typically, it was about 1/10 of the volume of the low pH buffer and sample). The use of neutralization solutions prepared in this way ensured that, except for the identity of the buffer salt, all samples were identical at the end of the pH treatment. In the ELISA, therefore, any pH dependence of antibody-antigen interactions (other than that due to irreversible pH-induced conformational changes in the antigen) was eliminated.

ELISA. A capture ELISA method was adopted to analyze the effects of pH treatment. In this method a rabbit anti-FMDV antiserum was used to capture antigen which was then detected by using a guinea pig anti-FMDV serum. Both antisera were prepared by injecting animals with A5 Allier/France 1960, A22 Iraq 24/64, and A24 Cruzeiro (Brazil 1955) by methods described previously (56) and were capable of binding to the three viral subtypes used in this study. Microtiter plates (96 wells) were prepared 24 h in advance by being coated with a 1/5,000 dilution of rabbit antiserum in 50 mM sodium carbonate-bicarbonate buffer (pH 9.6) at 4°C. Plates were washed with PBS immediately before use. Following pH treatment and neutralization, samples were diluted in PBS containing 0.1% (vol/vol) Tween 20 (PBS-Tween) to an antigen concentration of 0.07 to 0.3 μg/ml, and 50 μl was applied to each well in the coated plates. After 1 h at 37°C, unbound antigen was washed off with PBS, 50 μl of a 1/1,000 dilution in PBS-Tween of guinea pig anti-A antiserum was added to the plate, and incubation was continued for another hour at 37°C. Unbound antibody was washed off with PBS, and 50 μl of a 1/1,000 dilution in PBS-Tween of anti-guinea pig antibody conjugated with horseradish peroxidase (DAKO Immunoglobulins) was added to the plate for a final hour of incubation at 37°C. Finally, the conjugated antibody was washed off with PBS, and the plate was developed by the addition of 50 μl of 0.4 mg *ortho*-phenylenediamine per ml–0.015% (vol/vol) H_2O_2 for 10 min at room temperature. The colorimetric reaction was quenched by the addition of 50 μl of 1.25 M H_2SO_4. The optical density at 492 nm (OD_{492}) of each well was determined with an ELISA reader.

Preliminary experiments indicated that high antigen concentrations resulted in saturation of the colorimetric reaction under our experimental conditions, leading to a shift in the observed pH sensitivity and an underestimate of acid lability. Below a limiting antigen concentration, estimated from experiments at 0.3 μg/ml, saturation was avoided. Measurements of pH sensitivity performed at or below 0.3 μg/ml gave identical results (data not shown).

Sedimentation analysis. Radiolabelled virions and empty capsids were prepared as described above. Prior to pH treatment, 380 μg of unlabelled carrier virus ($A10_{61}$) per ml was added to the labelled sample. Following pH treatment, a further 60 μg of carrier per ml was added. Labelled samples were centrifuged in 12 ml of 10 to 30% (wt/vol) sucrose gradients containing a 0.75-ml 45% sucrose cushion at 261,000 × *g* for 125 min at 12°C. The sucrose solutions were prepared in either buffer P or buffer T. The gradients were drained and divided into fractions of equal volume; 10-μl samples from each fraction were dried onto filter paper, and the radioactivity was determined after immersion in scintillant.

RESULTS

Polypeptide composition of natural empty capsids. A major surprise at the outset of this study was the finding that in natural empty capsids most of VP0 had cleaved into VP2 and VP4, both of which remained associated with the capsid (Fig. 1). ^{35}S-labelled empty capsids isolated from an infection of BHK-21 cells were analyzed by SDS-PAGE. Quantification of the polypeptide composition by optical densitometry of autoradiograms revealed that, typically, only 20 of a total of 60 VP0 molecules were uncleaved (Table 1). This composition was observed for natural empty capsids of all three subtypes (A10, A22, and A24) but contrasted with recombinant empty capsids expressed from vaccinia virus, which contained essentially

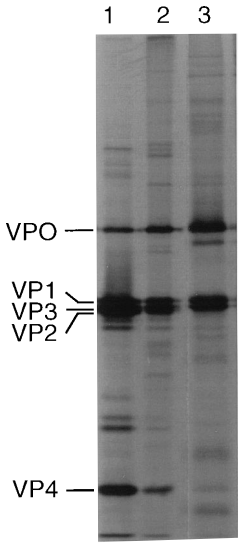

FIG. 1. Comparison of polypeptide compositions of virions and natural and recombinant empty capsids by SDS-PAGE. The samples shown are the peak fractions identified following sucrose gradient centrifugation of radiolabelled infected cell lyates prepared as described in Materials and Methods. Virus (lane 1) and natural empty capsids (lane 2) were isolated from BHK-21 cells infected with $A10_{61}$ FMDV. Recombinant empty capsids of type $A10_{61}$ FMDV (lane 3) were isolated from human TK^- cells infected with the vaccinia virus recombinants vTF7-3 and vT7CA2. The positions of the proteins are indicated on the left.

completely intact VP0 (Fig. 1). Although this result is not completely unprecedented for FMDV (61), other studies, using some of the same viral subtypes as those used here, found only negligible cleavage of VP0 in empty capsids (24, 59). We therefore investigated possible reasons for our observation.

It seemed possible that some or all of the empty capsids isolated might be a degradation product caused by whole virions losing their genomic RNA during the purification process. Therefore, purified radiolabelled virus was added to a monolayer of unlabelled, infected BHK-21 cells at the point of harvesting. The harvest was then subjected to the entire purification protocol for unlabelled virus (including ammonium sulfate precipitation, pelleting onto a sucrose cushion, and centrifugation through a sucrose gradient [see Materials and Methods]). As Fig. 2 shows, only whole labelled virions were recovered, demonstrating that empty capsids were not

TABLE 1. Effects of guanidine hydrochloride and EDTA on number of VP0 molecules per capsid remaining intact in FMDV $A10_{61}$ natural empty capsids

Drug	Concn (mM)	No. of Intact VP0 molecules/capsid[a]
Guanidine hydrochloride	0	16
	7	18
	14	20
	20	18
EDTA	0	17
Expt 1	1	19
	5	22
Expt 2	0	25
	25	27

[a] For details of the calculation, see Material and Methods.

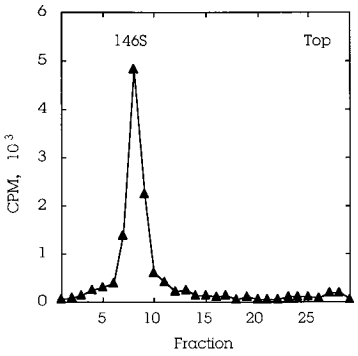

FIG. 2. Empty capsids are not derived from virions during purification. Purified, L-[^{35}S]methionine-labelled virus (strain $A10_{61}$) was added to unlabelled BHK-21 cells infected with the same virus at 4 h postinfection. The cells were immediately lysed, and the virus was purified as described for unlabelled material in Materials and Methods. In the final step of purification the virus was centrifuged on a 15 to 45% sucrose gradient. A portion of the original radiolabelled virus was centrifuged on a parallel gradient in order to identify the virus peak (data not shown).

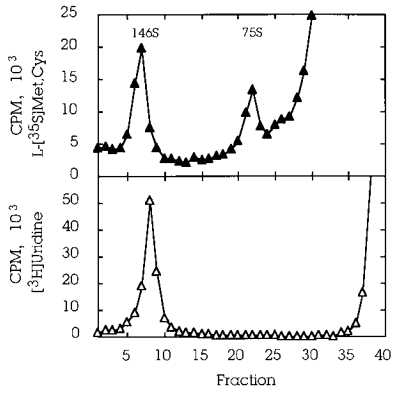

FIG. 3. Empty capsids contain negligible amount of RNA. BHK-21 cells infected with $A10_{61}$ FMDV were radiolabelled with [^{35}S]-Protein Labeling Mix at 2 h postinfection (filled triangles). At the same time an identical flask of BHK-21 cells infected with $A10_{61}$ FMDV in the presence of 1.25 μg of actinomycin D per ml was labelled with [^{3}H]uridine (open triangles). The cells were lysed after a further 2 h, and the lysate was analyzed on 10 to 30% sucrose gradients.

produced from virions by handling procedures. Even the addition of up to 25 mM EDTA at the point of cell lysis had no discernible effect on the proportion of VP0 molecules remaining intact in empty capsids (strain $A10_{61}$) (Table 1), thus reducing the likelihood that cellular proteases were responsible for cleavage.

Another possibility is that the natural empty capsids containing partially cleaved VP0 are derived from a labile population of virions with a similarly partial VP0 content which is lost during purification. However, no such particles, to our knowledge, have ever been reported for wild-type picornaviruses. In particular, no provirion like the one described for poliovirus (19), which contains both RNA and fully intact VP0, has been reported for FMDV. Moreover, one would reasonably expect that virions containing partially cleaved VP0 would be more thermostable than the corresponding empty capsids and that they should therefore have been detected.

The mechanism of VP0 cleavage in picornaviruses remains to be elucidated. Structural studies of HRV 14 led to the suggestion that cleavage occurs autocatalytically, with serine 10 of VP2 being the catalytic nucleophile and the viral RNA contributing to its activation (3). Experimental tests of this hypothesis have cast doubt on its validity. Although the mutation with serine 10 replaced by alanine depresses VP0 cleavage in HRV 14 (40), it does not abolish it altogether. In poliovirus, changing the equivalent serine to alanine or cysteine has no effect on VP0 cleavage (34). Nevertheless, we tested for a possible role of viral RNA in cleaving VP0 in FMDV empty capsids. Identical flasks of BHK-21 cells infected with $A10_{61}$ FMDV were labelled with either ^{35}S-Protein Labeling Mix or [^{3}H]uridine, and the cell lysate (harvested upon attaining >80% CPE) was centrifuged on sucrose gradients to separate the virions and empty capsids (Fig. 3) The RNA present in virions was clearly labelled. A negligible amount of labelled RNA was detected in empty capsids. By comparison with virions (8.5-kb RNA), an upper limit of 27 bases of RNA was calculated as the RNA content of empty capsids. This demonstrates that natural empty capsids were well resolved from virions on sucrose gradients and that the observed cleavage of VP0 is unlikely to be due to contamination by virions or defective interfering particles.

Following the observation that cleavage of VP0 in empty capsids of HRV was abolished by the addition of 3 mM guanidine hydrochloride to infected cultures (60), the effect of this drug on FMDV empty capsids was analyzed. At low concentrations (<20 mM), guanidine specifically inhibits viral RNA synthesis during infections by FMDV and other picornaviruses (4, 8, 14, 54) and has no effect on the level of protein synthesis in uninfected BHK-21 cells (data not shown). Its ability to abolish VP0 cleavage in HRV empty capsids supports the contention that RNA is involved in the cleavage event. BHK-21 cells infected with $A10_{61}$ FMDV were treated with 0, 7, 14, and 20 mM guanidine at 2 h postinfection. After 15 min, L-[^{35}S]methionine was added, and the infection products were harvested by cell lysis at full CPE, usually 6 h postinfection. The lysate was centrifuged to separate virus and empty capsids (Fig. 4). Suppression of viral RNA synthesis is evident from the observation that the recovery of labelled virions decreases with increasing guanidine concentration. As a consequence, the radiolabel was increasingly found incorporated into fractions containing empty capsids. At 7 mM guanidine the amount of labelled empty capsid recovered was approximately twice that in the absence of the drug. Beyond 14 mM guanidine the recovery of labelled empty capsids dropped off, possibly because of a reduction in the number of positive-strand RNA

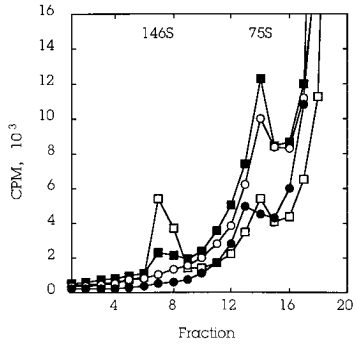

FIG. 4. Effect of guanidine hydrochloride on recovery of virions and empty capsids from infected BHK-21 cells. Identical flasks of cell monolayers were treated with 0 (open squares), 7 (closed squares), 14 (open circles), and 20 (closed circles) mM guanidine at 2 h postinfection. After 15 min, equal amounts of [^{35}S]methionine were added to each flask. The cells were lysed at 6 h postinfection and analyzed on 15 to 45% sucrose gradients.

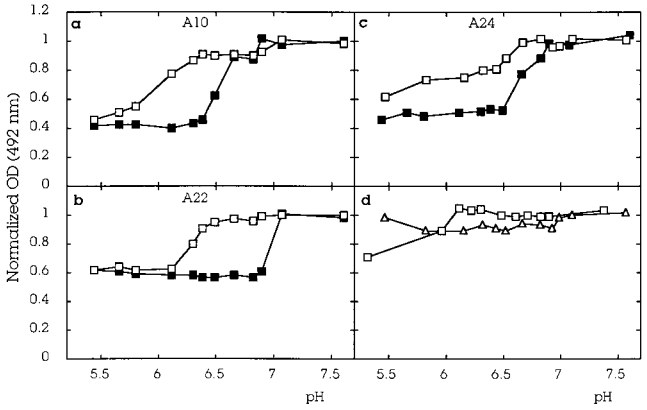

FIG. 5. Analysis of pH sensitivities of FMDV virions and empty capsids by ELISA. Equal concentrations of purified virus or empty capsids were diluted into 50 mM phosphate buffers containing 50 mM NaCl prepared at a range of pH values. After 8 min of incubation, the pH was restored to 7.6, and the samples were analyzed by ELISA as described in Materials and Methods. OD_{492} readings were normalized relative to the readings obtained at pH >7.0. (a to c) Virus (closed squares) and natural empty capsids (open squares) of $A10_{61}$ (a), A22 Iraq 24/64 (b), and A24 Cruzeiro (c). (d) Recombinant empty capsids expressed from double-recombinant vaccinia virus as described in Materials and Methods. The data shown for recombinant empty capsids were obtained at two ionic strengths, 50 mM (open squares) and 250 mM (open triangles) NaCl.

molecules reaching ribosomes. Alternatively, it may be that concentrations of guanidine in excess of 14 mM are interfering with correct capsid protein folding. Peak fractions containing empty capsids were analyzed by SDS-PAGE. The polypeptide composition of the empty capsids obtained at each concentration of the drug was determined by optical densitometry of the autoradiogram of the gel. As shown in Table 1, the VP0 content was unaffected by concentrations of guanidine up to 20 mM. In contrast to HRV empty capsids therefore, FMDV empty capsids are unaffected by this drug. This suggested that processing of VP0 in natural empty capsids of FMDV was not, as in HRV, dependent on viral RNA synthesis.

Analysis of acid lability of FMDV virions and empty capsids by ELISA. The acid dissociation of virus to pentamers was studied in detail by using a capture ELISA. The method makes use of the fact that, although the external surface of the FMDV pentamer displays virtually the entire antigenicity of the intact virion (18, 20), its ability to react in a capture ELISA is sterically limited. The resulting reduction in ELISA signal (56) thus provided a convenient and sensitive way of monitoring the disassembly process. Equal weights of virion (or natural or recombinant empty capsids) were diluted in buffers spanning a pH range of 5.3 to 7.6. After an incubation of 8 min, the pH of the sample was restored to 7.6, and the sample was applied to 96-well microtiter plates for analysis by ELISA as described in Materials and Methods. As the pH decreased, the ELISA reading (OD_{492}) dropped from a high to a low plateau level (Fig. 5a to c). The half-way point in this transition (pH_{50}) was taken as a measure of the pH sensitivity. Subsequent experiments (see below) confirmed that the drop in the ELISA reading results from conversion of the capsid (146S or 75S) into 12S pentamers.

Unexpectedly, for the three viral subtypes used in this study, there were clear differences in the pH of transition (Fig. 5; Table 2) Thus, virus A22 Iraq 24/64 was the least resistant to low pH, with a pH_{50} of 7.0 (Fig. 5b). In contrast, A24 Cruzeiro was observed to have a pH_{50} of 6.65 (Fig. 5c) and was marginally less stable at low pH than was $A10_{61}$ (Fig. 5a), which has a pH_{50} of 6.5. Increasing the concentration of NaCl from 50 to 250 mM in the pH buffers, thus raising the ionic strength, protected these viruses at low pH. The pH of transition was shifted by between −0.3 and −0.4 pH units (Table 2).

TABLE 2. pH_{50} values for virions and natural empty capsids of type A FMDV by ELISA

Particle	Subtype	pH_{50}[a]	
		50 mM NaCl	250 mM NaCl
Virus	A10	6.5	6.15
	A22	7.0	6.6
	A24	6.65	6.25
Natural empty capsid	A10	6.0	5.8
	A22	6.3	6.2
	A24	6.35	6.5

[a] The pH_{50} is defined as the pH at which the ELISA signal is half-way between the high (146S capsid) and low (12S pentamer) plateau levels (see Fig. 5).

Curiously, in $A10_{61}$ and A24 Cruzeiro, the transition from 146S to 12S occurred over a relatively broad range of pH (approximately 0.4 pH unit). In further experiments, setting the time of incubation of $A10_{61}$ virions to 4, 8, 16, or 24 min was found to have no observable effect on the range of pH over which the transition occurred (data not shown).

In all cases the natural empty capsids appeared significantly more resistant to low pH than the corresponding virion (Fig. 5). The pH of transition of the empty capsid was between 0.3 and 0.7 pH units lower than that of the virion (Table 2). Since virions and empty capsids (in this study) differ essentially only by RNA content, this observation suggests a key role for the genomic RNA in rendering virions more sensitive to pHs below 7.

In further contrast to virions, increasing the ionic strength of the pH buffer by raising the NaCl concentration from 50 to 250 mM had only a small protective effect on $A10_{61}$ and A22 Iraq 24/64 natural empty capsids. For A24 Cruzeiro empty capsids, high ionic strength was found reproducibly to destabilize the capsids by 0.15 pH units (Table 2).

The use of ELISA to analyze the effects of low pH on recombinant empty capsids ($A10_{61}$) produced results which were difficult to interpret (Fig. 5d). At 50 mM NaCl there was no significant variation in the OD_{492} over the pH range of 7.6 to 5.5, in contrast to that for natural empty capsids. At 250 mM NaCl there was an indication of a transition occurring at about pH 6.0, which was comparable to the observations for natural empty capsids under similar conditions. Sedimentation analysis helped to resolve this apparently paradoxical result.

Analysis of acid lability by sucrose gradient centrifugation. Sedimentation analysis of $A10_{61}$ FMDV was used to identify the nature of the conformational transition detected in the ELISA. As previously reported for virions (13), low pH resulted in a clear transition to a very slowly sedimenting species, namely 12S pentamers (Fig. 6). There was no evidence of any intermediate on the gradient. Likewise, empty capsids were also found to convert to 12S pentamers, albeit at lower pH values than for virions. Again no intermediate was detected. For both virions and natural empty capsids the conversion to 12S pentamers occurs over essentially the same range of pH as the transition observed in ELISA experiments. Moreover, Fig. 6c shows that at pH 6.0 only pentamers remain. Since there is no significant variation in the ELISA signal obtained with virus over the range pH 6.3 to 5.3 (Fig. 5a), the low plateau level observed in the ELISA experiments is due

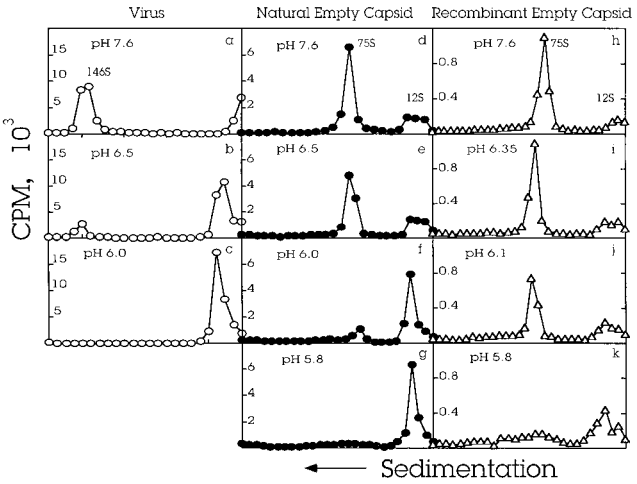

FIG. 6. Analysis of pH sensitivities of FMDV virions and empty capsids by centrifugation on sucrose gradients. Samples of purified virions and natural and recombinant empty capsids were diluted in 9 volumes of buffers prepared at a range of pH values. After 8 min, the pH was restored to pH 7.6, and the samples were centrifuged on 10 to 30% sucrose gradients. (a to c) $A10_{61}$ virus; (d to g) $A10_{61}$ natural empty capsids; (h to k) $A10_{61}$ recombinant empty capsids.

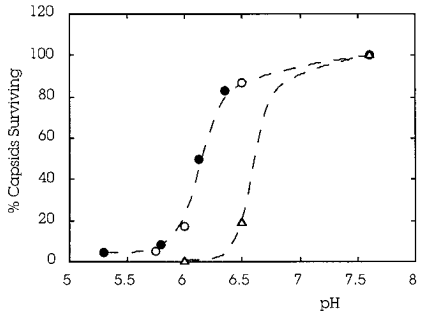

FIG. 7. Titration of dissociation of virions and empty capsids of FMDV $A10_{61}$ at low pH as determined by sedimentation analysis. The amount of virus (open triangles) and natural (open circles) and recombinant (closed circles) empty capsids remaining intact at each pH value examined was calculated as a fraction of the amount recovered after treatment at pH 7.6 (see the text). The curves fitted to the data by interpolation are drawn as a guide.

solely to pentamers. Thus the transition of the ELISA signal as the pH falls is due to dissociation of whole capsids into pentamers. Our data do not exclude the possibility that an intermediate particle is generated during the transition, but they dictate that it would exist only over a very narrow range of pH and would have the same sedimentation coefficient in sucrose as intact capsids. The occurrence of such an intermediate seems unlikely. While the capsids of picornaviruses such as poliovirus or rhinovirus are conformationally altered but not dissociated following heat or acid treatment or exposure to cellular receptors (27, 36, 37, 39, 43), FMDV is invariably reported to dissociate directly into pentamers following treatment by heat (23, 61) or acid (13) or upon internalization by susceptible cells (6).

In the case of recombinant empty capsids, although the ELISA results were difficult to interpret, it is clear from the sedimentation analysis that the capsids are degraded at low pH. However, the accumulation of 12S material is much less marked. It may be that dissociating recombinant empty capsids have a greater tendency to aggregate than natural empty capsids. When virus capsids dissociate at acidic pH, the myristylated protein VP4 separates from the pentamers and aggregates (13), possibly because of the presence of the myristyl moiety. In the recombinant empty capsids the myristate on VP0 remains associated with the pentamer and may therefore be implicated in aggregation. This notion is consistent with the observation that the ELISA signal for recombinant empty capsids remained high even as the pH was lowered since a captured aggregate might be expected to present many more antigenic sites that a single captured pentamer.

For virions, natural empty capsids, and recombinant empty capsids, the percentage of capsids surviving intact at each pH was calculated from sedimentation data. The results of these calculations are combined in Fig. 7, which shows that the pH sensitivities of empty capsids and recombinant empty capsids are indistinguishable. The plot also illustrates that the virus is about 0.5 pH unit more acid sensitive than the empty capsids, a difference that is indistinguishable from that measured by ELISA (Fig. 5; Table 2). The pH values at which conversion to 12S pentamers is 50% complete are slightly higher than the pH_{50} values determined from the ELISA experiments. This is probably due to the fact that the OD_{492} in the transition region results from contributions from both pentamers and intact capsids; because intact capsids bind the capture antibody with greater avidity, at the pH at which conversion to pentamers is 50% complete the ELISA reading is higher than the average for the upper (intact capsids) and lower (pentamers) plateaux, which is the definition of pH_{50}.

DISCUSSION

Mechanism of VP0 cleavage. Since VP2 and VP4 are usually found only in mature virions, it has been argued that interaction of the viral RNA with the nascent capsid somehow triggers the cleavage of VP0 (3). A detailed mechanism for this event has been proposed for picornaviruses in which a conserved serine residue is activated for nucleophilic attack on the peptide bond between VP2 and VP4 by the viral RNA (3). Although the three-dimensional structure of FMDV casts doubt on this hypothesis (2) and experiments to mutate the serine to an inactive group in poliovirus (34) and rhinovirus (40) suggest that this residue does not participate in cleavage, the possibility that RNA is required remains an open and attractive hypothesis. Comparison of the crystal structures of virions and empty capsids of poliovirus showed that cleavage of VP0 releases the N terminus of VP2 and the C terminus of VP4 to participate in the formation of a β-sheet which extends across the interface between two pentamers and conceivably contributes to capsid stability (28). The cleavage of VP0 may therefore be a mechanism for locking the RNA within the capsid. The most recent evidence suggests that VP0 cleavage may also be required to confer infectivity on picornaviruses (7, 40, 48).

The results of the experiments reported here suggest that cleavage of VP0 in FMDV can be decoupled from RNA encapsidation. Such a decoupling is also consistent with the results of a study of a mutant poliovirus which was defective for VP0 cleavage but still capable of encapsidating RNA (19). We found a negligible amount of RNA in the natural empty capsids isolated from infection of BHK-21 cells (Fig. 3). Moreover, the suppression of viral RNA synthesis by guanidine completely failed to protect the VP0 in empty capsids from cleavage (Fig. 4; Table 1). This latter finding contrasts with work on HRV empty capsids in which guanidine was shown to have a protective effect (60). However, it remains true that a greater degree of VP0 cleavage is observed in mature virions of FMDV than in empty capsids. Moreover,

empty capsids derived from a vaccinia virus recombinant which would not have been exposed to the complete RNA genome during assembly contained largely intact VP0. Both these observations are consistent with the view that viral RNA promotes VP0 cleavage. It may be that FMDV empty capsids arise from abortive attempts to encapsidate viral RNA: a partially completed capsid in which VP0 cleavage is initiated may dissociate from the RNA and become an empty capsid, as pentamers containing intact VP0 complete the capsid structure. Further work is required to elucidate both the mechanism of VP0 cleavage and the reasons for its occurrence in FMDV empty capsids.

The fact that VP0 is generally found to be uncleaved in empty capsids of poliovirus and rhinovirus, in contrast to our results with FMDV, may reflect structural differences on the interior of the capsids between these picornaviruses. It is more difficult to account for the discrepancy between our findings with $A10_{61}$ FMDV empty capsids and those of Rowlands et al. (59), who observed a much smaller degree of VP0 cleavage in the same viral subtype. Our methods differed in no significant respect from those of Rowlands and his colleagues. We were able to demonstrate that the natural empty capsids recovered in our experiments were not produced by mishandling of virions in our purification procedure. Moreover, using a similar purification protocol, we recovered recombinant empty capsids from the vaccinia virus recombinant without a significant degree of VP0 cleavage (Fig. 1). From this evidence it seems unlikely that our results are artefactual.

Mechanism of virus uncoating. FMDV is the most sensitive of all the picornaviruses to acidic pH. Our results confirm this sensitivity but highlight that it varies between viral subtypes which differ by only about 10% in the amino acid sequence of their capsid proteins. The range of variation for the three subtypes in this study is 0.5 pH unit. Such variation is clearly not problematic for virion growth, as might be expected for an infection pathway depending on acidification within the endosome where the pH can be as low as 5.0 (47). However, an acid-resistant mutant of A12 FMDV, selected after exposure to pH 6.4, does have a small plaque phenotype and is released more slowly from infected cells (12), suggesting that acid-sensitive viruses are better adapted for rapid replication.

We have measured the difference in the acid stabilities of virions and natural and recombinant empty capsids. For all three subtypes the natural empty capsids are significantly more resistant to acid-induced dissociation into pentamers than the corresponding virions (Table 2), consistent with the observations of Graves et al. (32). Recombinant empty capsids of FMDV $A10_{61}$ were shown to have the same acid lability as natural empty capsids of the same subtype (Fig. 7), indicating that cleavage of VP0 has no effect on acid stability. Thus the increased acid lability of virions compared with that of empty capsids arises from the presence of viral RNA. This finding is all the more surprising given that RNA encapsidation is associated with increased thermostability of picornavirus capsids (23, 57).

The effect of RNA in modulating pH sensitivity may be due to RNA-protein interactions or a nonspecific dielectric effect of the nucleic acid. The crystal structures of the virion and natural empty capsid of A22 Iraq FMDV (22) show that the packing of the capsid proteins relative to one another is identical in both particles. The empty capsids differ from virions only in features which are confined to the internal face of the capsid. Thus the N termini of VP1 and VP2 and the C terminus of VP4 are all more disordered in the empty capsid than in the virion. In the virion structure the C terminus of VP4 and the N-terminal portion of VP2 that is visible (the first 11 residues are disordered in the virus and are not included in the model) pack directly against the RNA. The N terminus of VP1 packs underneath the C terminus of VP4. Since VP0 is largely cleaved into VP2 and VP4 in natural empty capsids, the disordering observed is most likely due simply to the absence of RNA. It is conceivable that in the presence of RNA in the mature virion the ordering of these termini, which are close to one another and overlie the interpentamer interface, brings together titratable amino acids which may be responsible for the increased acid lability of the virion. However, if this is the case, it remains unclear from the structure which groups are involved.

Alternatively, it may be that the effect of RNA on the dielectric environment of the capsid is primarily responsible for the difference in acid sensitivities of virions and empty capsids. Electrostatic interactions between titratable groups are the most likely determinants of pH sensitivity, and the value of the dielectric constant of the medium (protein, nucleic acid, or solvent) surrounding such groups affects the strength of these interactions. High dielectric constants reduce the energy of electrostatic interactions. Thus RNA might destabilize the FMDV capsid by, for example, displacing the aqueous solvent, which has a relatively high dielectric constant, from the vicinity of key amino acids.

Structural studies on acid effects in picornaviruses have focussed on HRV and mengo virus, which are conformationally altered at pH values around 5.0 and 6.2, respectively. At low pH, HRV undergoes a transition to a form which appears very similar to the intermediate generated by interaction of the virus with susceptible cells (39). Acid-stable mutants of HRV 14 contain mutations clustered in the vicinity of a depression in the virus surface (31, 63), which is the attachment site of the cellular receptor, ICAM-1 (50). The mutations appear to protect the virus at low pH by increasing the stability of the capsid (31), but the groups responsible for triggering the acid-induced conformational change have yet to be identified.

In striking contrast to HRV, neither mengo virus nor FMDV converts to an intermediate form at low pH; they dissociate directly into pentamers (13, 44). Crystallographic analyses of mengo virus under different conditions of pH and ionic strength have implicated the GH loop of VP1 and the C terminus of VP2, both of which contain His residues, in the acid-induced dissociation of the capsid (38). These investigators (38) propose that pH-induced movements of these features displace a phosphate ion at the icosahedal 2-fold axis; this reduces the neutralization of positive charges on either side of the pentamer interface leading to dissociation of the capsid.

The pentamer interface of FMDV is the most likely location of residues which determine sensitivity to acidic conditions because of the observation that low pH induces dissociation into pentameric subunits. As has already been noted, this interface is rich in histidine residues which have a pK_a of 6.8 in solution (2). Since A22 FMDV is between 0.4 and 0.5 pH units more sensitive to acidic conditions than A10 or A24, sequence comparisons between these subtypes might allow us to identify more precisely those parts of the interface which are responsible for modulating pH sensitivity. An examination of a preliminary model of the FMDV A22 crystal structure (22) reveals several sequence differences between the three subtypes at the pentamer interface (Table 3), a number of which correlate with pH sensitivity (i.e., the amino acid found in A10 and A24 differs from that found at the corresponding position in the more acid-labile FMDV A22).

A subset of these changes was clustered at the middle of the interface, close to the icosahedral twofold-symmetry axis (Fig. 8). At this location there is an α-helix formed by residues 89 to

TABLE 3. Sequence differences between A22, A10, and A24 FMDV at the pentamer interface[a]

FMDV subtype	Residue at position indicated									
	VP2							VP3		
	65	88	91	98	110	191	192	70	71	139
A22	H	K	Y	F	S	T	V	E	Q	K
A10	F	H	F	Y	C	N	T	D	T	E
A24	Y	H	F	Y	S	N	T	D	T	R

[a] Sequence data for A22, A10, and A24 were obtained from references 1, 9, and 17, respectively.

98 of VP2. Positioned 4Å from the N terminus of this helix, and hence from the positive end of the dipole associated with it, is the side chain of His-142 from VP3 of the 2-fold-related pentamer. Because of twofold symmetry, there are two copies of this histidine and α-helix arrangement at each pentamer interface. It is conceivable that protonation of His-142 in VP3, which is strictly conserved in FMDV (51), would give rise to repulsive electrostatic interactions across the interface which might lead to pentamer dissociation. Measurements on mutants of barnase indicate that protonation of a His at the N terminus of an α-helix destabilizes the protein by between 0.5 and 1.1 kcal (~4.6 kJ) mol^{-1} (62), although in that case the His is on the same polypeptide chain as the helix. The VP2 α-helix is conserved in other picornavirus structures, but FMDV is unique in placing a His residue at the positive end of the helix dipole. The histidine-helix dipole interaction may thus be an important determinant of the acid lability of FMDV. Conformational changes leading to the formation of pentamers in this region may be facilitated by the extensive hydration of the N-terminal region of the α-helix observed in a number of FMDV structures (22), and it is likely that other features in the vicinity of this interaction contribute to the pH-induced dissociation of the virus.

Our analysis reveals that there are two residue changes in this helix between A22 on the one hand and A10 and A24 on the other (Table 3; Fig. 8). The changes, relative to A22, are Tyr-91 to Phe and Phe-98 to Tyr. Both involve a difference in a polar group which may affect the stability of this region. The pockets containing the side chains of both these residues are strongly conserved within FMDV. Moreover, at the N terminus of the helix, Lys-88 of VP2 in FMDV A22 is replaced by a His in A10 and A24 (Fig. 8). Protonation of His-65 in VP2 of A22 may contribute to destabilization of the pentamer interface; A10 and A24 contain a Phe and a Tyr, respectively, at this position. At the icosahedral threefold-symmetry axis, where three pentamers come together, Thr-191 and Val-192 in VP2 of A22 are replaced by Asn-191 and Thr-192 in both A10 and A24. Residue 191 is highly exposed in the structures of A22 and A10 (22), although increased van der Waals contact between the larger Asn residue in A10 and A24 might contribute to stability. The replacement of Val-192 by Thr, a similarly sized residue, is a relatively conservative change and does not introduce H bonds between the threefold-symmetry-related Thr residues in A10 (22). It is noteworthy, however, that in type O FMDV, residues 191 and 192 of VP2 were identified as potential cation ligands (41). It may be that variation of these residues in A22 relative to A10 and A24 affects cation binding so as to render the virus more acid labile. Other sequence differences at the pentamer interface seem less likely to affect pH sensitivity. Near to the helices at the two-fold axis, for example, residue 139 in VP3 varies between the three subtypes (Lys in A22, Glu in A10, and Arg in A24), but these variations are difficult to correlate with the observed differences in pH sensitivity.

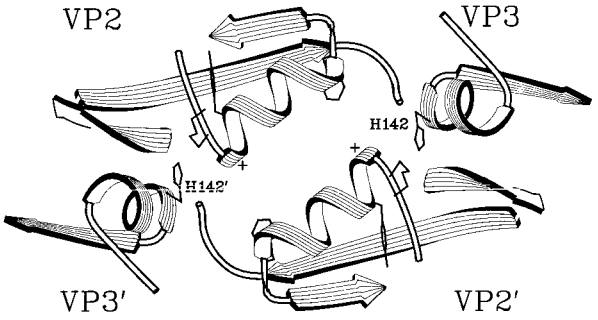

FIG. 8. Schematic representation of the histidine-helix dipole interaction between twofold-related pentamers in A22 FMDV. For simplicity, only portions of one copy of VP2 and VP3 from each of the two pentamers are shown. The pentamer interface passes horizontally through the center of the figure. Labels associated with the twofold-related pentamer are indicated by ′. The positive end of the helix dipoles are indicated by +. Side chains associated with the helix which vary between A22 and A10 and A24 as discussed in the text are shown (Lys-88, Tyr-91, and Phe-98). The diagram was produced by using SETOR (26).

Mutagenesis experiments are now required to test the role of the proposed histidine-helix dipole interaction in determining the pH sensitivity of FMDV and the possible modulation of that sensitivity by the sequence variation identified above.

ACKNOWLEDGMENTS

We thank Wendy Blakemore and Julia Brangwyn for superb technical assistance.

S.C. was supported by the BBSRC. This work was also supported by MAFF and by Commission of the European Communities contract B10T-CT90-0190. D.I.S. is a member of the Oxford Centre for Molecular Sciences.

REFERENCES

1. **Abrams, C.** 1993. Ph.D. thesis. Reading University, United Kingdom.
2. **Acharya, R., E. Fry, D. Stuart, G. Fox, D. Rowlands, and F. Brown.** 1989. The three-dimensional structure of foot-and-mouth disease virus at 2.9Å resolution. Nature (London) **337:**709–716.
3. **Arnold, E., M. Luo, G. Vriend, M. G. Rossmann, A. C. Palmenberg, G. D. Parks, M. J. H. Nicklin, and E. Wimmer.** 1987. Implications of the picornavirus capsid structure for polyprotein processing. Proc. Natl. Acad. Sci. USA. **81:**21–25.
4. **Baltimore, D.** 1968. Inhibition of poliovirus replication by guanidine, p. 340–347. *In* M. Saunders and E. H. Lennette (ed.), Medical and applied virology. Warren H. Green, Inc., St. Louis, Mo.
5. **Baxt, B.** 1987. Effect of lysomotropic compounds on early events in foot-and-mouth disease virus replication. Virus Res. **7:**257–271.
6. **Baxt, B., and H. L. Bachrach.** 1980. Early interactions of foot-and-mouth disease virus with cultured cells. Virology **104:**42–55.
7. **Bishop, N. E., and D. A. Anderson.** 1993. RNA-dependent cleavage of VP0 capsid protein in provirions of hepatitis A virus. Virology **197:**616–623.
8. **Black, D. N., and F. Brown.** 1969. Effect of actinomycin D and guanidine on the formation of a ribonucleic acid polymerase induced foot-and-mouth disease virus and on the replication of virus and viral ribonucleic acid. Biochem. J. **112:**317–323.
9. **Bolwell, C., A. L. Brown, P. V. Barnett, R. O. Campbell, B. E. Clarke, N. R. Parry, E. J. Ouldridge, F. Brown, and D. J. Rowlands.** 1989. Host cell selection of antigenic variants of foot-and-mouth disease virus. J. Gen. Virol. **70:**45–57.
10. **Brown, F., and B. Cartwright.** 1961. Dissociation of foot-and-mouth disease virus into its nucleic acid and protein components. Nature (London) **192:** 1163–1164.
11. **Brown, F., and B. Cartwright.** 1963. Purification of radioactive foot-and-mouth disease virus. Nature (London) **199:**1168–1170.
12. **Brown, F., T. Twomey, J. F. E. Newman, T. Burrage, and S. Hassard.** 1993. Abstracts of the 9th International Congress of Virology, abstr. P19–19, Glasgow.
13. **Burroughs, J. N., D. J. Rowlands, D. V. Sangar, P. Talbot, and F. Brown.** 1971. Further evidence for multiple proteins in the foot-and-mouth disease

virus particle. J. Gen. Virol. **13:**73–84.
14. **Caliguiri, L. A., and I. Tamm.** 1968. Action of guanidine on the replication of poliovirus RNA. Virology **35:**408–417.
15. **Carrillo, E. C., C. Giachetti, and R. H. Campos.** 1984. Effect of lysosomotropic agents on the foot-and-mouth disease virus replication. Virology **135:** 542–545.
16. **Carrillo, E. C., C. Giachetti, and R. H. Campos.** 1985. Early steps in FMDV replication: further analysis on the effects of chloroquine. Virology **147:**118–125.
17. **Carroll, A. R., D. J. Rowlands, and B. E. Clarke.** 1984. The complete nucleotide sequence of the RNA encoding for the primary translation products of foot-and-mouth disease virus. Nucleic Acids Res. **12:**2461–2472.
18. **Cartwright, B., W. G. Chapman, and F. Brown.** 1980. Serological and immunological relationship between the 146S and 12S particles of foot-and-mouth disease virus. J. Gen. Virol. **50:**369–375.
19. **Compton, S. R., B. Nelsen, and K. Kirkegaard.** 1990. Temperature-sensitive poliovirus mutant fails to cleave VP0 and accumulates provirions. J. Virol. **64:**4067–4075.
20. **Crowther, J. R., C. A. Rowe, and R. Butcher.** 1993. Characterisation of monoclonal antibodies against a type SAT-2 foot-and-mouth disease virus. Epidemiol. Infect. **111:**391–406.
21. **Curry, S., R. Abu-Ghazaleh, W. Blakemore, E. Fry, T. Jackson, A. King, S. Lea, D. Logan, J. Newman, and D. Stuart.** 1992. Crystallization and preliminary X-ray analysis of three serotypes of foot-and-mouth disease virus. J. Mol. Biol. **228:**1263–1268.
22. **Curry, S., E. Fry, and D. I. Stuart.** Unpublished data.
23. **Doel, T. R., and P. J. Baccarini.** 1981. Thermal stability of foot-and-mouth disease virus. Arch. Virol. **70:**21–32.
24. **Doel, T. R., and W. K. T. Chong.** 1982. Comparative immunogenicity of 146S, 75S and 12S particles of foot-and-mouth disease virus. Arch. Virol. **73:**185–191.
25. **Dunnebacke, T. H., J. D. Levinthal, and R. C. Williams.** 1969. Entry and release of poliovirus as observed by electron microscopy of cultured cells. J. Virol. **4:**505–513.
26. **Evans, S. V.** 1990. SETOR: hardward lighted three-dimensional solid model representation of macromolecules. J. Mol. Graphics **11:**134–138.
27. **Fenwick, M. L., and P. D. Cooper.** 1962. Early interactions between poliovirus and ERK cells: some observations on the nature and significance of the rejected particles. Virology **18:**212–223.
28. **Flore, O., C. E. Fricks, D. J. Filman, and J. M. Hogle.** 1990. Conformational changes in poliovirus assembly and cell entry. Semin. Virol. **1:**429–438.
29. **Fricks, C. E., and J. M. Hogle.** 1990. Cell-induced conformational change in poliovirus: externalization of the amino terminus of VP1 is responsible for liposome binding. J. Virol. **64:**1934–1945.
30. **Fuerst, T. R., E. G. Niles, W. Studier, and B. Moss.** 1986. Eukaryotic transient-expression system based on recombinant vaccinia virus that synthesizes bacteriophage T7 RNA polymerase. Proc. Natl. Acad. Sci. USA **83:** 8122–8126.
31. **Giranda, V. L., B. A. Heinz, M. A. Oliveira, I. Minor, K. H. Kim, P. R. Kolatkar, M. G. Rossmann, and R. R. Rueckert.** 1992. Acid-induced structural changes in human rhinovirus 14: possible role in uncoating. Proc. Natl. Acad. Sci. USA **89:**10213–10217.
32. **Graves, J. H., K. M. Cowan, and R. Trautman.** 1968. Immunochemical studies of foot-and-mouth disease virus. II. Characterisation of RNA-free virus-like particles. Virology **34:**269–274.
33. **Gromeier, M., and K. Wetz.** 1990. Kinetics of poliovirus uncoating in HeLa cells in a nonacidic environment. J. Virol. **64:**3590–3597.
34. **Harber, J. J., J. Bradley, C. W. Anderson, and E. Wimmer.** 1991. Catalysis of poliovirus VP0 cleavage is not mediated by serine 10 of VP2. J. Virol. **65:** 326–334.
35. **Hogle, J. M., M. Chow, and D. J. Filman.** 1985. Three-dimensional structure of poliovirus at 2.9Å resolution. Science **229:**1358–1365.
36. **Hummeler, K., and V. V. Hamparian.** 1958. Studies on the complement fixing antigans of poliomyelitis. I. Demonstration of type and group specific antigens in native and heated viral preparations. J. Immunol. **81:**499–505.
37. **Joklik, W. K., and J. E. Darnell.** 1961. The adsorption and early fate of purified poliovirus in HeLa cells. Virology **13:**439–477.
38. **Kim, S., U. Boege, S. Krishnaswamy, I. Minor, T. J. Smith, M. Luo, D. G. Scraba, and M. G. Rossmann.** 1990. Conformational variability of a picornavirus capsid: pH-dependent structural changes of mengo virus related to its host receptor attachment site and disassembly. Virology **175:**175–190.
39. **Korant, B. D., K. Lonberg-Holm, J. Noble, and J. T. Stasny.** 1972. Naturally occurring and artificially produced components of three rhinoviruses. Virology **48:**71–86.
40. **Lee, W.-M., S. S. Monroe, and R. R. Rueckert.** 1993. Role of maturation cleavage in infectivity of picornaviruses: activation of an infectosome. J. Virol. **67:**2110–2122.
41. **Logan, D.** 1992. Ph.D. thesis. Oxford University, Oxford.
42. **Luo, M., G. Vriend, G. Kamer, I. Minor, E. Arnold, M. G. Rossmann, U. Boege, D. G. Scraba, G. M. Duke, and A. C. Palmenberg.** 1987. The atomic structure of mengo virus at 3.0Å resolution. Science **235:**182–191.
43. **Madshus, I. H., S. Olsnes, and K. Sandvig.** 1984. Requirements for entry of poliovirus RNA into cells at low pH. EMBO J. **3:**1945–1950.
44. **Mak, T. W., D. J. O'Callaghan, and J. S. Colter.** 1970. Studies of the pH inactivation of three variants of mengo encephalomyelitis virus. Virology **40:** 565–571.
45. **Marsh, M., and A. Helenius.** 1989. Virus entry into cells. Adv. Virus. Res. **36:**107–151.
46. **Mason, P. W., B. Baxt, F. Brown, J. Harber, A. Murdin, and E. Wimmer.** 1993. Antibody-complexed foot-and-mouth disease virus, but not poliovirus, can infect normally insusceptible cells via the Fc receptor. Virology **192:**568–577.
47. **Mellman, I., R. Fuchs, and A. Helenius.** 1986. Acidification of the endocytic and exocytic pathways. Annu. Rev. Biochem. **55:**663–700.
48. **Moscufo, N., A. Gomez Yafal, A. Rogove, J. Hogle, and M. Chow.** 1993. A mutation in VP4 defines a new step in the late stages of cell entry by poliovirus. J. Virol. **67:**5075–5078.
49. **Neubauer, C., L. Frasel, E. Kuechler, and D. Blaas.** 1987. Mechansim of entry of human rhinovirus 2 into HeLa Cells. Virology **158:**255–258.
50. **Olson, N. H., P. R. Lolatkar, M. A. Oliveira, R. H. Cheng, J. M. Greve, A. McClelland, T. S. Baker, and M. G. Rossmann.** 1993. Structure of human rhinovirus complexed with its receptor. Proc. Natl. Acad. Sci. USA **90:**507–511.
51. **Palmenberg, A. C.** 1989. Sequence alignments of picornaviral capsid proteins, p. 211–241. *In* B. L. Semler and E. Ehrenfeld (ed.), Molecular aspects of picornaviral infection and detection. American Society for Microbiology, Washington, D.C.
52. **Pérez, L., and L. Carrasco.** 1993. Entry of poliovirus into cells does not require a low-pH step. J. Virol. **67:**4543–4548.
53. **Prchla, E., E. Kuechler, D. Blaas, and R. Fuchs.** 1994. Uncoating of human rhinovirus 2 from late endosomes. J. Virol. **68:**3713–3723.
54. **Pringle, C. R.** 1964. Inhibition of multiplication of foot-and-mouth disease virus by guanidine hydrochloride. Nature (London) **204:**1012–1013.
55. **Randrup, A.** 1954. Ultracentrifugation of the virus of foot-and-mouth disease. IV. Splitting of the greater complement-fixing particle. Acta Pathol. Microbiol. Scand. **34:**366–374.
56. **Roeder, P. L., and P. M. Le Blanc Smith.** 1987. Detection and typing of foot-and-mouth disease virus by enzyme-linked immunosorbent assay: a sensitive, rapid and reliable technique for primary diagnosis. Res. Vet. Sci. **43:**225–232.
57. **Rombaut, B., K. Andries, and A. Boeyé.** 1991. A comparison of WIN51711 and R78206 as stabilisers of poliovirus virons and procapsids. J. Gen. Virol. **72:**2153–2157.
58. **Rossmann, M. G., E. Arnold, J. W. Erickson, E. A. Frankenberger, J. P. Griffith, H. J. Hecht, J. E. Johnson, G. Kamer, M. Luo, A. G. Mosser, R. R. Rueckert, B. Sherry, and G. Vriend.** 1985. Structure of a human common cold virus and functional relationship to other picornaviruses. Nature (London) **317:**145–153.
59. **Rowlands, D. J., D. V. Sangar, and F. Brown.** 1975. A comparative chemical and serological study of the full and empty particles of foot-and-mouth disease virus. J. Gen. Virol. **26:**227–238.
60. **Rueckert, R. (University of Wisconsin).** 1992. Personal communication.
61. **Rweyemamu, M. M., G. Terry, and T. W. F. Pay.** 1984. Stability and immunogenicity of empty particles of foot-and-mouth disease virus. Arch. Virol. **59:**69–79.
62. **Sancho, J., L. Serrano, and A. R. Fersht.** 1992. Histidine residues at the N- and C-termini of α-helices: perturbed pK_as and protein stability. Biochemistry **31:**2253–2258.
63. **Skern, T., H. Torgersen, H. Auer, E. Kuechler, and D. Blaas.** 1991. Human rhinovirus mutants resistant to low pH. Virology **183:**757–763.
64. **Warwicker, J.** 1992. Model for the differential stabilities of rhinovirus and poliovirus to mild acidic pH, based on electrostatics calculations. J. Mol. Biol. **223:**247–257.
65. **Willingmann, P., H. Barnert, H. Zeichhardt, and K.-O. Habermehl.** 1989. Recovery of structurally intact and infectious poliovirus type 1 from HeLa cells during receptor-mediated endocytosis. Virology **168:**417–420.
66. **Zeichhardt, H., K. Wetz, P. Willingmann, and K.-O. Habermehl.** 1985. Entry of poliovirus type 1 and mouse Elberfeld (ME) virus into HEp-2 cells: receptor-mediated endocytosis and endosomal or lysosomal uncoating. J. Gen. Virol. **68:**483–492.